Int J Clin Exp Med 2016;9(8):15414-15425
www.ijcem.com /ISSN:1940-5901/IJCEM0021562

Original Article

Chronopharmacodynamics of gefitinib-based anti-cancer effect in Lewis tumor-bearing mice

Bin Zhang[1*], Yanqin Cheng[2*], Xiujie Fang[3], Qing Lu[2], Jiao Liu[2], Guoxin Liu[2], Peipei Wang[2], Liang Liu[2], Pingping Lin[2], Mingchun Li[2]

[1]Chinese Academy of Medical Sciences & Peking Union Medical College, Institute of Medicinal Plant Development (IMPLAD), Beijing 100193, China; [2]Department of Pharmacy, The 401st Hospital of Chinese People's Liberation Army, Qingdao, Shandong 266071, China; [3]Beijing Dongcheng Community Health Service Center, Beijing 100010, China. [*]Equal contributors.

Received December 10, 2015; Accepted March 19, 2016; Epub August 15, 2016; Published August 30, 2016

Abstract: Gefitinib is a tyrosine kinase inhibitor in the fight against NSCLC by inhibiting intracellular phosphorylation of tyrosine kinase associated with the epidermal growth factor receptor. To explore the influence of different dosing times on the efficacy and toxicities of gefitinib and the underlying mechanism, a mouse model of Lewis lung carcinoma was established in C57BL/6 mice. The tumor and skin tissues were observed with scanning electron microscopy. In addition, the levels of IL-6 and TNF-α, phosphorylation level of EGFR and ERK1/2, and mRNA expressions of EGFR, ABCG2, and MMP-9 were determined by ELISA, Western-blot and qRT-PCR technique, respectively. The present study found administration of gefitinib at 8:00 and 4:00 significantly inhibited the tumor growth, and IL-6 and TNF-α levels were higher between 16:00 and 24:00 than at 8:00. Meanwhile, the level of pEGFR and pERK1/2 was higher at 16:00 and 20:00. The cells apoptosis induced by gefitinb administered at 8:00 was more aggravating compared with administration at 16:00. These findings indicate that efficacy and toxicities of gefitinib vary with the time of day of administration. The molecular mechanism of action may be related to dynamic activity of EGFR-RAS-RAF-ERK1/2 pathway. Accordingly, the time of gefitinib administration should be taken into consideration in clinic.

Keywords: Gefitinib, NSCLC, EGFR, circadian rhythm, tumor, lung cancer

Introduction

Lung cancer, which leads to 1.38 million annual deaths worldwide, is the most common causation of cancer mortality in men and the second most common cause in women [1]. The 5-year survival rate of this disease for all stages is only 15% [2]. There into, non-small-cell lung cancer (NSCLC) accounts for 80% of all the types of lung cancer. Although most NSCLC patients can benefit from chemotherapy, the platinum-based first-line therapy can only bring about median survival times of 8 to 11 months, with 1- and 2-year survival rates being 35-40% and 10-20%, respectively [3, 4]. Furthermore, poor prognosis and disease progression are inevitable, and simultaneously severe cytotoxicities confine these drugs' utilization. Therefore, it is extremely urgent to search for a more effective method to treat NSCLC.

In the past decades, great progress has been made in the exploration of signal transduction pathways. Epidermal growth factor receptor (EGFR) is a member of erbB family of transmembrane receptors tyrosine kinase, which is over-expressed in many solid tumors, including head and neck, non-small cell lung and prostate cancers [5]. Activation of EGFR by ligand binding can promote tumor proliferation, angiogenesis, invasion and metastasis [6]. Therefore, inhibiting EGFR pathways might be a promising strategy in the treatment of advanced NSCLC. In all of EGFR-targeted agents, gefitinib (IRESSA), an orally administered small molecular targeted drug, is a typical representative. As a targeted therapeutic agent, gefitinib has demonstrated its clinical advantage in the treatment of advanced NSCLC patients who have previously received platinum-based chemotherapy, especially females, never-smokers, and those with adenocarcinoma histology [7, 8]. The mechanism of this drug is that it can reversibly bind the ATP pocket in the EGFR intracellular tyrosine kinase domain and inhibit its tyrosine kinase [9].

Biological rhythms, existing naturally from unicellular organisms to complex mammalians, synchronize organisms' physiological, biochemical, metabolic and behavioral processes with changes in the external environment, to guarantee the organisms to accommodate, anticipate, and respond to the changes effectively [10]. Based on the biological rhythms, it has been put forward that cancer might be caused by circadian-related disorders [11]. Moreover, recent researches have interpreted that many behaviors of both normal cells and tumor cells in mammals show a characteristic 24-hour circadian rhythm of their growth, proliferation, DNA synthesis, and secretion activities [12-16]. As most chemotherapeutic agents not only inhibit the malignant cells but impair normal healthy cells, the therapeutic effect of the drugs should be weighed against their toxicities. Hence, optimizing the dosing time of the drugs according to the circadian rhythm plays a critical role in maximizing their anti-tumor efficacy and in decreasing their adverse reactions. The efficacy of some antimetabolites, such as platinum drugs (cisplatin, carboplatin, and oxaliplatin), 5-fluorouracil, and doxorubicin, has displayed notable circadian rhythm [17-19]. The basis for these drugs might be the differences in the biological rhythmicity of proliferation and DNA synthesis between normal healthy cells and malignant cells. However, as a small molecular targeted agent, gefitinib is completely distinct from the above drugs in the anticancer mechanism. What's more, no relevant researches have been reported in the field of chronotherapy. So identifying its circadian rhythm is meaningful to the cancer patients and will help to achieve better chronopharmacotherapy for NSCLC treatment.

The purpose of this study was to investigate the influence of gefitinib on the inhibition of tumor growth at different times in mice and the underlying mechanism. We aim to find a proper time for chemotherapy to provide the reference to the clinical treatment.

Materials and methods

Mice, cells and reagents

C57BL/6 female mice (aged 5 weeks 18-20 g) were purchased from Vital River Laboratory Animal Technology Co. Ltd (Beijing, China). The mice were housed in common animal lab in groups of 5 per cage under standardized light-dark cycle conditions (lights (501 ×) on from 7:00 to 19:00) at a room temperature of 24±1°C and a humidity of 60±10% with food and water available ad libitum. The mice were accommodated to the light/dark cycle for one week before the experiments. All animal experiments were conducted in accordance with the Bioethics Committee guidelines in the 401st Hospital of Chinese People's Liberation Army.

The Lewis lung carcinoma cells (ATCC, CRL-1642) were bought from Beijing Chuanglian North Carolina Biotechnology Research Institute. The cells were then cultured with Dulbecco's modified Eagle's medium (Hyclone laboratories Inc USA) containing 10% fetal bovine serum, 1% penicillin, and 1% streptomycin (Hyclone laboratories Inc USA) in a 37°C humidified incubator with 5% CO_2 atmosphere. A total of 0.2 ml of 1×10^6 viable tumor cells was injected into the left hind footpad of each mouse. One week later, evident implanted tumors were observed.

Gefitinib (AstraZeneca UK Limited) was provided by the 401st Hospital of Chinese People's Liberation Army. The tablets were stored at room temperature and dissolved in distilled water with 5% sodium carboxymethylcellulose before application. To observe its therapeutical effect, the drug was given to tumor-bearing mice via intragastric administration (100 mg/kg).

Experiment design

The tumor-bearing mice were randomly allocated into 7 groups (n = 10), including the Model group, experimental groups 8:00, 12:00, 16:00, 20:00, 24:00, and 4:00. The mice in the 6 experimental groups were given via gavage a single dose of gefitinib (100 mg/kg), and those in the Model group were treated with the same volume of 5% sodium carboxymethylcellulose. The experiment was performed for three weeks. On the 22nd day, the mice in experimental and Model groups were killed with their tumor pelt off at 8:00, 12:00, 16:00, 20:00, 24:00, and 4:00, respectively.

Tumor volume assessment

The length and width diameters of the tumors of each mouse were measured with vernier caliper every three days during the experiments. The tumor volume was calculated as shown in **Eq 1** [20].

Tumor volume (cm^3) = $A \times B^2/2$ (**Eq 1**)

where A is the length diameter and B is the width one (centimeter).

Tumor weight and tumor inhibition rate

After three weeks' treatment, the mice were killed by cervical dislocation. Their tumors were pelt off in sterile conditions and weighed. The tumor inhibition rate was calculated as shown in **Eq 2** [21],

$$\text{Tumor hibition rate}(\%) = \frac{\text{Average tumor weight of control group} - \text{Average tumor weight of treament group}}{\text{Average tumor weight of control group}} \times 100\%$$

(**Eq 2**)

ELISA analysis of TNF-α and IL-6 levels

The blood samples were collected from the eye socket vein of the mice after three weeks' treatment with the drug. TNF-α and IL-6 levels in the blood were determined by ELISA kit (Biolegend Inc.) according to the manufacturer's recommendations. The absorbance of the samples was read on the microplate reader (BIO-TEK Elx-800/808) at 450 nm.

Scanning electron microscopy (SEM)

In preparation for SEM, the tumor and skin tissues were cut with a razor blade into many small blocks. Afterwards the block specimens were completely rinsed in a 0.1 M phosphate buffer solution (PBS), fixed in 2.5% glutaraldehyde for a few hours, and postfixed in 1% OsO_4 in PBS. Next, they were dehydrated in a graded series of ethanol solutions, immersed in isoamyl acetate, and critical-point-dried in CO_2. Finally, they were ion-sputtered with palladium and observed via a scanning electron microscopy (Hitachi Ltd. S-4800, Japan).

qRT-PCR analysis

The expression levels of EGFR, ABCG2 (ATP-binding cassette sub-family G member 2), MMP-9 (matrix metalloproteinase-9), and GAPDH were determined by qRT-PCR technique. The total mRNA was extracted with RNAiso Plus (Takara Biotechnology (Dalian) Co., Ltd.) according to the manufacture's instruction. cDNA was synthesized from 2 μl total RNA using PrimeScript(R) RT reagent Kit (Takara Biotechnology (Dalian) Co., Ltd.). The qRT-PCR analyses were performed using TL989 Real Time Quantitative PCR (Xi'an Tianlong Science and technology Co., Ltd). The primers of the above genes were designed and synthesized by Takara Biotechnology (Dalian) Co., Ltd based on the principles for prime design by UCSC. The primers sequences and cycling conditions of each gene were displayed in **Table 1**.

Protein extraction and western blot

Frozen tumor tissues were transferred into mortar, and then crushed with pestle to homogenize until powdery after the adding of liquid nitrogen. According to the amount of tissue powder, appropriate ice-cold lysis buffer (50 mM Tris-HCl, pH 7.8, 150 mM NaCl, 5 mM EDTA, 0.5% Nonidet P-40, 2 mM PMSF, 1 mM Na_3VO_4) was added, and then the homogeneous tissue was cultured on ice for 30 min. After the removal of the insoluble materials by centrifugation at 12,000 g for 10 min at 4°C, the protein concentrations in tumor mass lysates were determined using a bicinchoninic acid protein assay kit (CWBIO, China), and the resulting supernatants were mixed with an 1/5 volume of 5 × sample buffer and boiled at 95°C for 5 min. Equal amounts of proteins (10 μl/well) were separated using 10% SDS-polyacrylamide gels electrophoresis and then transferred to PVDF membrane (Millipore, US). Subsequently, the membranes were incubated overnight at 4°C with antibodies against β-actin, total EGFR (tEGFR), phospho-EGFR (pEGFR), total ERK1/2(tERK1/2), phospho-ERK1/2, bax and bcl-2 (monoclonal rabbit anti-mouse antibodies 1:1000; Cell Signaling Technology, US) at 4°C. Then the membranes were incubated with horseradish peroxidase-conjugated secondary antibodies (Rabbit IgG, 1:6000; Cell Signaling Technology, US). The images from the immunoreactive membrane were digitized. Protein band intensities were quantified using NIH Image software.

TUNEL assay

DNA fragmentation in situ was detected by TUNEL assay according to the kit instructions (Roche, Germany). 4',6-diamidino-2-phenylindole (DAPI) was included in the kit as DNA fragments could be stained by TUNEL specifically and produced green fluorescence, while DAPI could combine with complete DNA and debris and produced blue fluorescence. Briefly, tissue sections were fixed with 4% paraformaldehyde at room temperature, and then rinsed with PBS for 5 min and incubated in a permeabilization solution (1% Triton X-100 in 0.1% sodium

Table 1. RT-qPCR primer sequences and cycling conditions for each gene

Genes	Prime sequence	Accession NO.	Cycling conditions	Number of cycles
EGFR	F: GTAGTGAGCTGAGGGCTTTACTGG	NM_207655.2	1. 30 s 2. 5 s 30 s 60 s	Process 2 with 40 cycles
	R: TCAGGGATGGATAACGGTTAGG			
ABCG2	F: ACGACTGGTTTGGACTCAAGCAC	NM_011920.3	1. 30 s 2. 5 s 30 s 30 s	Process 2 with 35 cycles
	R: AAAGATGGAATACCGAGGCTGATG			
MMP-9	F: GCCCTGGAACTCACACGACA	NM_013599.2	1. 30 s 2. 5 s 30 s 60 s	Process 2 with 40 cycles
	R: TTGGAAACTCACACGCCAGAAG			
GAPDH	F: TGTGTCCGTCGTGGATCTGA	NM_008084.2	1. 30 s 2. 5 s 30 s 60 s	Process 2 with 40 cycles
	R: TTGCTGTTGAAGTCGCAGGAG			

citrate) for 2 min on ice. The TUNEL reaction mixture was added and the samples were incubated for 1 h at 37°C humidified atmospheres (5% CO_2) in the dark and then dyed with 1 μg/ml of DAPI for 15 min. After rinsing with PBS, samples were analyzed under a fluorescence microscope using an excitation wavelength in the range of 450-500 nm and detection in the range 515-565 nm. The apoptotic rate was indicated by percentage of the TUNEL-positive cell number against the total cell number (DAPI-positive) within the same area from five random selected fields in each treatment.

Statistical analysis

All statistical analyses were accomplished using SPSS 19.0 (SPSS Inc., Chicago, IL). All quantitative data were expressed as Mean ± SD and analyzed using one-way ANOVA and LSD (Least-significant difference), while the comparison between rates was carried out by χ^2 test. A value of $P < 0.05$ was set as statistically significant.

Results

Influence of gefitinib dosing times on tumor volume

Figure 1A shows the influence of dosing times on the gefitinib inhibition on tumor growth. The tumor growth displayed significant differences among groups in which gefitinib administered at different time points. Three weeks later, the minimum average tumor volume was detected in group 8:00. The volume was smaller than the Model, groups 16:00 ($P < 0.01$, LSD). The tumor in group 4:00 also showed a small volume, but was bigger than group 8:00 on average ($P > 0.05$).

Influence of gefitinib dosing times on tumor weight and tumor inhibition rate

The tumor inhibition rate of each group is displayed in **Table 2**, which exhibits marked differences among different gefitinib groups ($\chi^2 = 36.00$, $P = 0.000$). Group 8:00 showed the maximum tumor inhibition rate, and it was significantly higher than those of groups 16:00, 20:00, and 24:00 ($P < 0.05$, χ^2 test). However, the tumor inhibition rate was insignificantly different among groups 16:00, 20:00, and 24:00 ($P > 0.05$).

Influence of gefitinib dosing times on TNF-α and IL-6 levels in blood

Both IL-6 and TNF-α production in the blood were significantly augmented in the treatment groups when compared with those in the Model group (**Figure 2A**, **2B**). Treatment with gefitinib at 8:00 can relatively normalize the IL-6 production. The secretion of IL-6 was markedly increased in the mice which were given gefitinib at the other times, particularly at 16:00 and 20:00 (**Figure 2A**). Also, TNF-α level in group

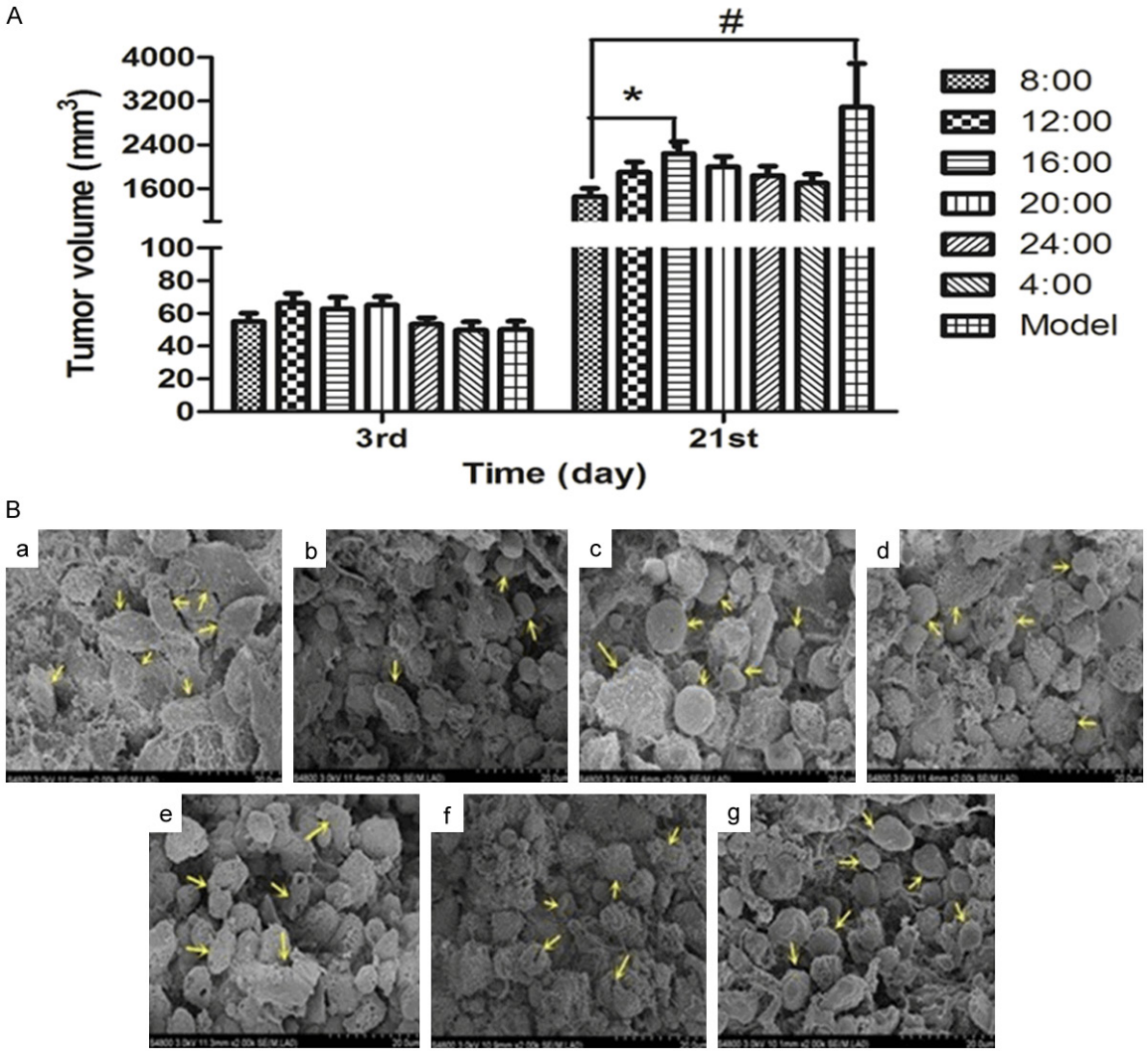

Figure 1. The antitumor effect of gefitinib treated at 8:00 was enhanced compared to those were given at other time points. The tumor volume was determined after 3 weeks treatment (A) and Lewis lung carcinoma cells were observed by SEM (B). Pictures Ba-g were from groups 8:00, 12:00, 16:00, 20:00, and 24:00 and Model group, respectively. The arrow in picture pointed to abnormal deformation of cells, with fibrotic substances covered. *P < 0.05 compared to group 16:00, #P < 0.01 as compared to Model group (LSD).

Table 2. Tumor weight and tumor inhibition rate in mice from various groups

Groups	Tumor weight (g)	Tumor inhibition rate
8:00	3.04±0.62	44.12%
12:00	3.62±1.74	33.46%
16:00	4.67±2.04	14.15%
20:00	4.22±1.17	22.43%
24:00	4.43±1.02	18.57%
4:00	3.35±1.37	38.42%
Model	5.44±1.57	

8:00 was significantly lower than that in groups 16:00 (P < 0.05, **Figure 2B**).

Observation of tumor and skin tissues by SEM

As is shown in **Figure 1B**, obvious differences in the appearance of Lewis lung carcinoma cell surfaces were observed, including their number, distribution, and morphology of microvilli. The biggest number of the tumor cells was observed in the Model group (**Figure 1Bg**), and their arrangement was extremely tight. No conspicuous deformation was noticed. The distribution of cells in **Figure 1Ba** was excessively irregular, with large amounts of deformation of cells. The surfaces of these cells were highly unsmooth. Although the number of the tumor cells in **Figure 1Bf** exceeded that in **Figure 1Ba**,

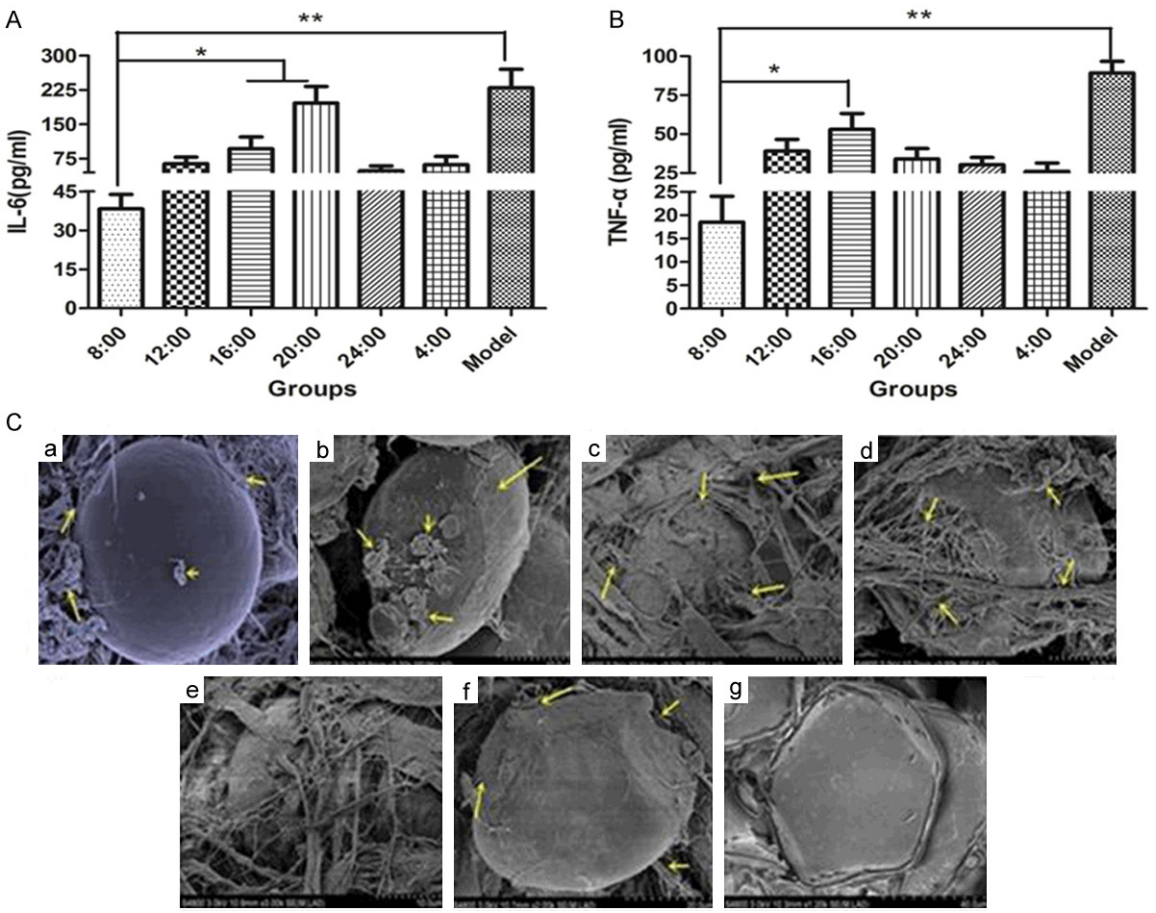

Figure 2. The adverse effects of gefitinib were relatively attenuated when given at 8:00. The IL-6 (A) and TNF-α (B) level in the blood of tumor-bearing mice were determined. Skin cells in tumor bearing mice were observed by SEM (C). Pictures Ca-g were from groups 8:00, 12:00, 16:00, 20:00, and 24:00 and Model group, respectively. The yellow arrow marked the fibrosis parts. *$P < 0.05$ compared to group 16:00, **$P < 0.01$ compared to the Model group (LSD).

microvilli on their surface were much more than those in **Figure 1Bb-e**.

There was significant distinction in the skin tissues among the seven groups (**Figure 2C**). The cell surface in **Figure 2Ca** was a little rougher than that in **Figure 2Cg**, in which the cell surface was extremely smooth and bright. The situations were even worse in **Figure 2Cb-e**, where some fibrosis appeared. The most serious was found in **Figure 2Cc**, in which the skin cells were completely covered by the fibrous substances. The results imply that the impairment by gefitinib to the normal skin might be less when administered at 8:00.

Gene expressions of EGFR, ABCG2, MMP-9 in tumor bearing mice

As shown in **Figure 3A**, the mRNA expression of EGFR in various groups exhibited insignificant differences ($P > 0.05$) for the over-expression of EGFR in all of the tumor-bearing mice.

ABCG2, the gene related to the transportation of gefitinib, was determined. There were no obvious distinction among groups 8:00, 12:00, and 16:00 ($P > 0.05$, **Figure 3B**). The mRNA expression of ABCG2 in group 20:00 was upregulated by twice when compared with that in group 8:00 ($P < 0.05$, LSD).

To observe the influence of gefitinib given at different times on the tumor metastasis, the mRNA expression of MMP-9 was measured because it was found over-expressed in many advanced NSCLC patients [22-25]. As shown in **Figure 3C**, the mRNA expression of MMP-9 in group 20:00 was increased by 3.20 and 3.32 folds when compared to groups 8:00 and 4:00, respectively ($P < 0.05$, LSD).

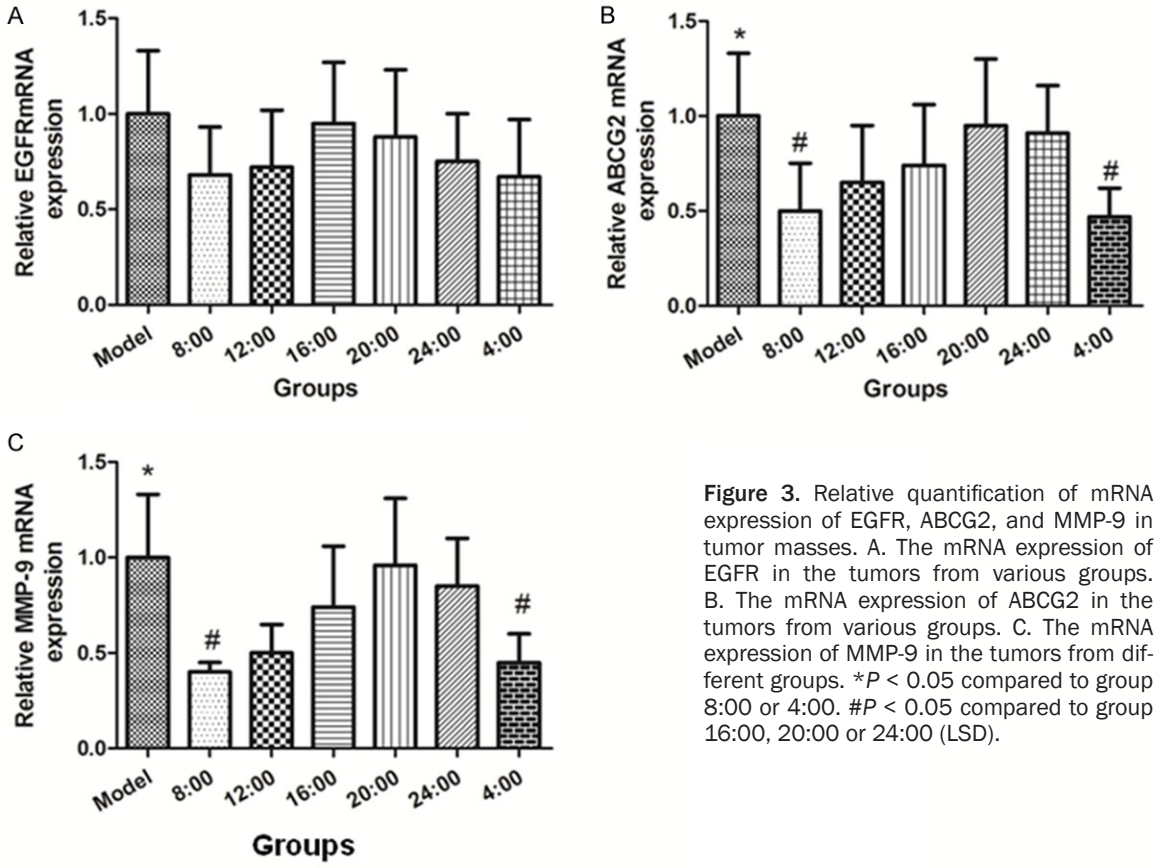

Figure 3. Relative quantification of mRNA expression of EGFR, ABCG2, and MMP-9 in tumor masses. A. The mRNA expression of EGFR in the tumors from various groups. B. The mRNA expression of ABCG2 in the tumors from various groups. C. The mRNA expression of MMP-9 in the tumors from different groups. *P < 0.05 compared to group 8:00 or 4:00. #P < 0.05 compared to group 16:00, 20:00 or 24:00 (LSD).

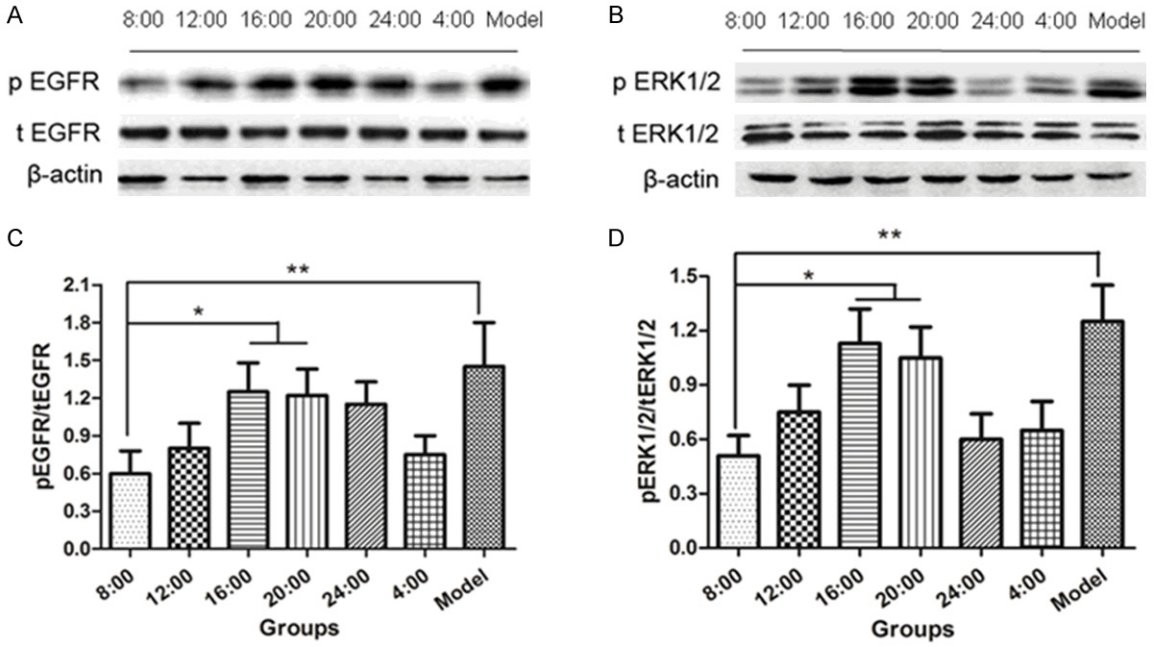

Figure 4. Influence of dosing times on tEGFR, pEGFR, tERK1/2, and pERK1/2 protein expression in tumor masses. A. Western blot analysis of β-actin, tEGFR and pEGFR protein expression in the tumor. B. Western blot analysis of β-actin, tERK1/2, and pERK1/2 protein expression. C. Relative pEGFR protein expression in the tumor tissues after geftinib (100 mg/kg) administration. D. Relative pERK1/2 protein expression in the tumor tissues from various groups treated by gefitinib (100 mg/kg) at different time points. *P < 0.05 compared to group 16:00 or 20:00, **P < 0.01 compared to the Model group (ANOVA).

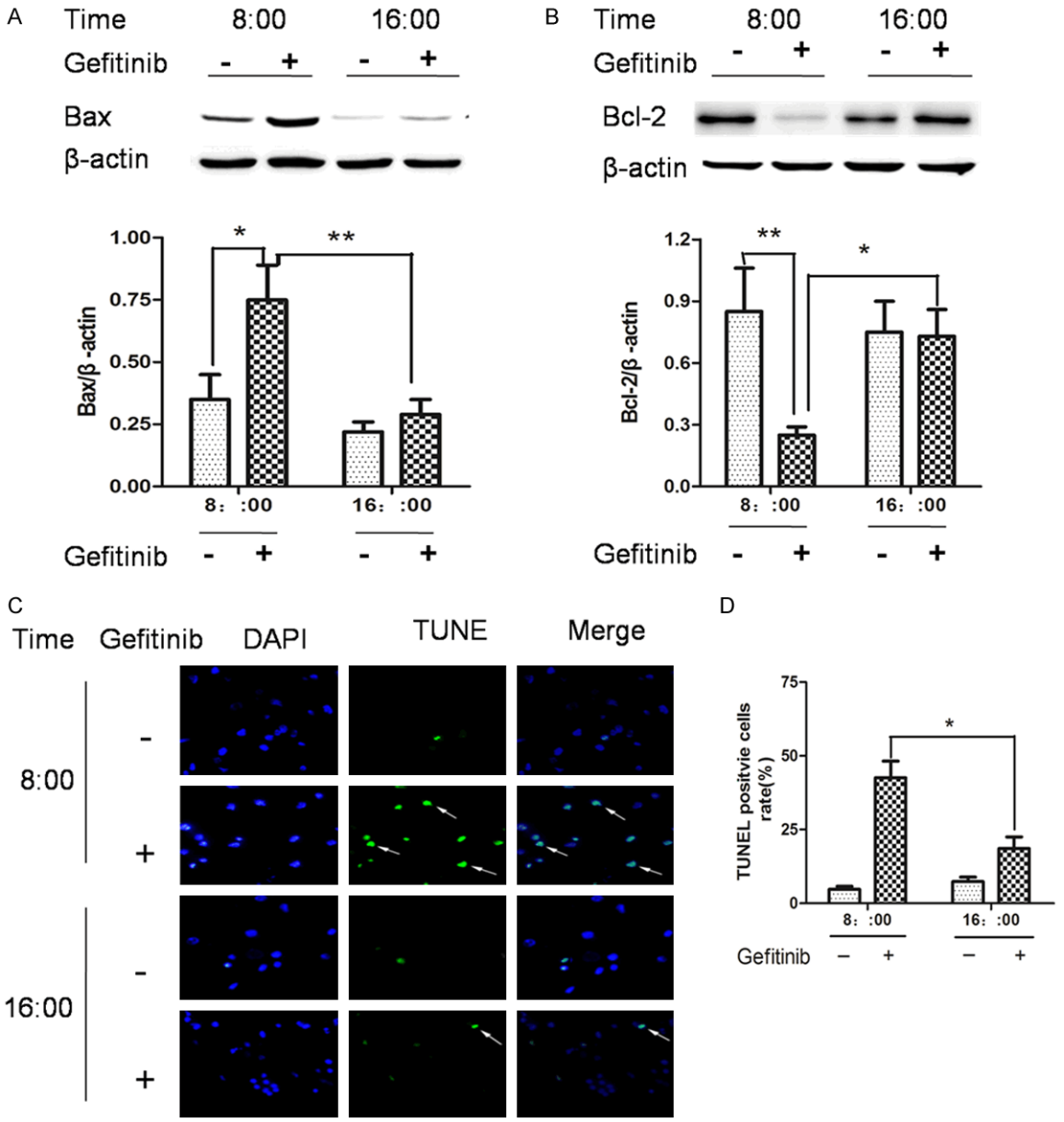

Figure 5. Influence of administration time on the ability of gefitinib to aggravate Lewis lung carcinoma cells apoptosis. A, B. Western blot analysis of β-actin, bax and bcl-2 protein expression in the tumor. C. Fluorescence microscopy images of TUNEL staining. Arrows represent TUNEL-positive cells. D. The quantitative analysis of TUNEL-positive cells rate. *$P < 0.05$, **$P < 0.01$ when compared between groups (ANOVA).

Influence of gefitinib dosing times on pEGFR and pERK1/2 protein levels

As shown in **Figure 4A**, the pEGFR protein level in groups 8:00 and 4:00 was significantly lower when compared with that in the Model group, groups 16:00 and 20:00 ($P < 0.05$, LSD). The phospho-ERK1/2 protein level was also measured (**Figure 4B**). It was found that pERK1/2 protein level in groups 16:00 and 20:00 was significantly higher than that in groups 8:00 and 4:00 ($P < 0.05$, LSD).

Influence of gefitinib dosing times on Lewis lung carcinoma cells apoptosis

Now that the anti-tumor effect of gefitinib was distinct when given at various time points, we mainly observed apoptotic level between group 8:00 and group 16:00. As shown in **Figure 5**, the expression of bax, a pro-apoptotic protein, was increased in group 8:00 compared with the group 16:00. Conversely, bcl-2, a anti-apoptotic protein was significantly decreased ($P < 0.05$, ANOVA). Also, the TUNEL assay results

were in accordance the former. Few TUNEL-positive cells were detected in the group 16:00, while TUNEL-positive cells increased dramatically in group 8:00 (18.32% and 43.65%, respectively).

Discussion

As a small molecular-targeted drug, gefitinib has been used for the treatment of advanced NSCLC, and its clinical efficacy has been improved by many researches on molecular biology, especially of cancer-related genes and proteins. Gefitinib is effective in treating NSCLC because it can reversibly and competitively inhibit the binding of adenosine triphosphate (ATP) to the phosphate-binding loop of the ATP site in the intracellular domain of EGFR. By inhibiting the binding of ATP to EGFR, the drug restrains auto-phosphorylation and the activation of downstream signaling pathway further, leading to the inhibition of cell proliferation and inducing apoptosis in NSCLC.

It was demonstrated in this study that the growth of Lewis lung carcinoma inoculated into C57BL/6 mice was inhibited by gefitinib and that the efficacy and adverse reactions of the agent varied with its different dosing time points. After three weeks of administration of gefitinib at certain time points, the tumor volume exhibited significant differences. The tumor sizes in group 8:00 were much smaller than those in groups 16:00, 20:00, and 24:00 ($P < 0.01$, LSD). The tumor inhibition rate in group 8:00 was significantly higher than that in groups 16:00 and 20:00 (44.12% vs. 14.15% and 22.43%, $P < 0.05$; **Table 2**), suggesting that administration of gefitinib at 8:00 can exert its maximum efficacy to inhibit tumor growth. In addition, 4:00 might be another proper time for administering gefitinib. Meanwhile, the tumor tissues in various experimental groups were analyzed by scanning electron microscopy. Morphological analysis about the cells by SEM revealed that the impairment induced by gefitinib to the tumor cells was much severer when the drug was given at 8:00 (**Figure 1Bb**), with irregular distribution and abnormal deformation. Furthermore, administration of gefitinib at 8:00 can promote tumor cells apoptosis more heavily than at 16:00 (**Figure 5**). These results collectively suggested that dosing gefitinib in the morning might be more effective.

ABCG2 (ATP-binding cassette sub-family G member 2), a plasma glycoprotein, provides physiological protection against xenobiotics, influences bio-distribution of drugs, and confers multidrug resistance to cancer cells. The accumulation of ABCG2 is in favor of the production of acquired resistance to gefitinib [26]. As over-expression of ABCG2 is a predictor for ill efficacy of gefitinib treatment [27], the ABCG2 expression in solid tumor was measured. The mRNA expressions of ABCG2 in groups 20:00 and 24:00 were extremely high (**Figure 3B**), suggesting that 8:00 might be suitable for administration of gefitinib without generating acquired drug resistance easily. In addition, the high mRNA expression of ABCG2, a main transport protein, between 20:00 and 24:00 indicates that the metabolism of gefitinib might be faster with short mean residence time (MRT), which wasn't beneficial to exert its best efficacy.

MMP-9 (matrix metalloproteinase-9), a member of the MMP family, plays a crucial role in degrading type IV collagen fibers and the extracellular matrix, which is closely related to metastasis and invasiveness [28]. MMP-9 may act as underlying prognostic and therapeutic markers in lung cancer, and high expression of MMP-9 means poor prognosis and low survival rate [29]. Hence, the mRNA expression of MMP-9 was determined to compare the influence of gefitinib on the solid tumors in each group. The mRNA expression of MMP-9 in groups 16:00 and 20:00 was increased by 3.20 and 3.32 folds when compared to groups 8:00 (**Figure 3C**), indicating that administration of gefitinib at 8:00 might result in better prognosis and higher survival rate.

Although typical adverse reactions induced by cytotoxic chemotherapy, such as hematological side effects, can be avoided when gefitinb is applied, cutaneous toxicities caused by gefitinib are still there, which directly affects treatment compliance and impinge on life quality of the patients [30, 31]. Rashes, one major result of cutaneous toxicities, can't be ignored, although it poses no threat on the life. Observation of skin tissues by SEM indicates that administration of gefitinb at 8:00 could prevent the skin cells from dehydration and fibrosis and could decrease the damage to skin tissues. Immunological mechanism of erlotinib-induced skin rashes has been reported to be positively

correlated to serum TNF-α and IL-6 levels [32]. Both TNF-α and IL-6 levels were determined in our study to estimate the impact of gefitinib on rashes. The TNF-α and IL-6 levels in various groups were in accordance with the results of skin tissues observed by SEM. The results indicate that more TNF-α and IL-6 were secreted at 16:00 and 24:00 than at 8:00 and 4:00 (**Figure 2**), hinting that cutaneous toxicities might be relatively decreased at these two time points.

Interleukin-6 (IL-6), a cytokine featuring pleiotropic activity, contributes to host defense against many a disease. IL-6 plays a significant role in the gastrointestinal tract, and is closely related to colorectal cancer [33]. In the gastrointestinal tract disorders, particularly diarrhea, the plasma level of IL-6 is elevated to modulate biological response to the disease [34]. Therefore, the IL-6 production in the tumor-bearing mice was detected to explore the injury to the gastrointestinal tract caused by gefitinib. All the groups showed extremely high level, especially in the Model group. The results suggest that the agent might have a weaker influence on the gastrointestinal tract when administered at 8:00.

At present the mechanisms of chronochemotherapy about gefitinib are still unclear. The target of gefitinib is EGFR and gefitinib can suppress the tumor growth by inhibiting EGFR autophosphorylation to block the downstream signal transduction. RAF, RAS and ERK1/2 are the downstream factors of EGFR signaling pathway. Some researches [35, 36] have reported ERK1/2 signal pathway is closely related to lung adenocarcinoma and plays a critical role in tumor cell proliferation. Based on the related findings, we investigated whether the EGFR-ERK signaling pathway was sensitive to the small molecular target TKI gefitinib. In this study, the mRNA expression of EGFR was found to have no significant differences (**Figure 3A**) because it was over-expression in the tumor. However, the proteins p-EGFR and p-ERK1/2 were found to exhibit circadian rhythm on different time points. The p-EGFR and p-ERK1/2 protein levels in groups 8:00 and 4:00 were significantly lower when compared with the Model, groups 16:00, and 20:00 (**Figure 4**), indicating better inhibition can be achieved to the EGFR signaling through EGFR-RAF-RAS-ERK1/2 pathway when gefitinib was administered at 8:00 and 4:00. Hence, it can be concluded the mechanism of chronochemotherapy of gefitinib might be related to the EGFR-RAS-RAF-ERK1/2 pathway.

Some shortcomings existed in our experiment. For example, the mouse model of Lewis lung carcinoma cells wasn't consummate for lack of experiments with lung cancer cell line with mutant EGFR. However, this part of research on a mouse model mutant target is being in progress. Secondly, the interstitial pneumonia was not monitored with an effective method. The interstitial pneumonia is a serious and lethal adverse reaction [37, 38], with a reported incidence of 4-6% in Japan and 0.3% in the USA among such parents [39]. Moreover, because it was difficult for us to observe the occurrence of rashes and diarrhea in the tumor bearing mice, we only determined the relevant cytokines to estimate the injuries to the skin and the gastrointestinal tract. Therefore, we carried out morphological analysis of skin cells by SEM in combination with determination of cytokines, TNF-α, and IL-6, to explore its cutaneous toxicities. However, our results are of great significance as a preliminary exploration in the field of small molecular targeted drugs.

In conclusion, this finding of present study reveals, for the first time, that the efficacy and toxicities of gefitinib vary with its dosing time during a day. Moreover, the time-dependent change in the sensitivity of Lewis lung cancer cells may be related to the EGFR-RAS-RAF-ERK1/2 signaling pathway. The time factor should be taken into account when gefitinib is clinically applied.

Disclosure of conflict of interest

None.

Address correspondence to: Dr. Mingchun Li, Department of Pharmacy, 401 Hospital of Chinese People's Liberation Army, 22 Min-Jiang Road, Qingdao 266071, Shandong, China. Tel: +86-532-51870086; Fax: +86-532-51872904; E-mail: lmc-401y@163.com

References

[1] Ferlay J, Shin HR, Bray F, Forman D, Mathers C and Parkin DM. Estimates of worldwide burden of cancer in 2008: GLOBOCAN 2008. Int J Cancer 2010; 127: 2893-2917.

[2] Schabath MB, Thompson ZJ and Gray JE. Temporal trends in demographics and overall survival of non-small-cell lung cancer patients at Moffitt Cancer Center from 1986 to 2008. Cancer Control 2014; 21: 51-56.
[3] Schiller JH, Harrington D, Belani CP, Langer C, Sandler A, Krook J, Zhu J, Johnson DH; Eastern Cooperative Oncology Group. Comparison of four chemotherapy regimens for advanced non-small-cell lung cancer. N Engl J Med 2002; 346: 92-98.
[4] Fossella F, Pereira JR, von Pawel J, Pluzanska A, Gorbounova V, Kaukel E, Mattson KV, Ramlau R, Szczesna A, Fidias P, Millward M and Belani CP. Randomized, multinational, phase III study of docetaxel plus platinum combinations versus vinorelbine plus cisplatin for advanced non-small-cell lung cancer: the TAX 326 study group. J Clin Oncol 2003; 21: 3016-3024.
[5] Salomon DS, Brandt R, Ciardiello F and Normanno N. Epidermal growth factor-related peptides and their receptors in human malignancies. Crit Rev Oncol Hematol 1995; 19: 183-232.
[6] Jorissen RN, Walker F, Pouliot N, Garrett TP, Ward CW and Burgess AW. Epidermal growth factor receptor: mechanisms of activation and signalling. Exp Cell Res 2003; 284: 31-53.
[7] Kim ES, Hirsh V, Mok T, Socinski MA, Gervais R, Wu YL, Li LY, Watkins CL, Sellers MV, Lowe ES, Sun Y, Liao ML, Osterlind K, Reck M, Armour AA, Shepherd FA, Lippman SM and Douillard JY. Gefitinib versus docetaxel in previously treated non-small-cell lung cancer (INTEREST): a randomised phase III trial. Lancet 2008; 372: 1809-1818.
[8] Giaccone G. Epidermal growth factor receptor inhibitors in the treatment of non-small-cell lung cancer. J Clin Oncol 2005; 23: 3235-3242.
[9] Fukuoka M, Yano S, Giaccone G, Tamura T, Nakagawa K, Douillard JY, Nishiwaki Y, Vansteenkiste J, Kudoh S, Rischin D, Eek R, Horai T, Noda K, Takata I, Smit E, Averbuch S, Macleod A, Feyereislova A, Dong RP and Baselga J. Multi-institutional randomized phase II trial of gefitinib for previously treated patients with advanced non-small-cell lung cancer (The IDEAL 1 Trial). J Clin Oncol 2003; 21: 2237-2246.
[10] Okamura H. Clock genes in cell clocks: roles, actions, and mysteries. J Biol Rhythms 2004; 19: 388-399.
[11] Sahar S and Sassone-Corsi P. Metabolism and cancer: the circadian clock connection. Nat Rev Cancer 2009; 9: 886-896.
[12] Levi F. Chronotherapeutics: the relevance of timing in cancer therapy. Cancer Causes Control 2006; 17: 611-621.
[13] Levi F, Okyar A, Dulong S, Innominato PF and Clairambault J. Circadian timing in cancer treatments. Annu Rev Pharmacol Toxicol 2010; 50: 377-421
[14] Eismann EA, Lush E and Sephton SE. Circadian effects in cancer-relevant psychoneuroendocrine and immune pathways. Psychoneuroendocrinology 2010; 35: 963-976.
[15] Huang XL, Fu CJ and Bu RF. Role of circadian clocks in the development and therapeutics of cancer. J Int Med Res 2011; 39: 2061-2066.
[16] Filipski E and Levi F. Circadian disruption in experimental cancer processes. Integr Cancer Ther 2009; 8: 298-302.
[17] Yang K, Zhao N, Zhao D, Chen D and Li Y. The drug efficacy and adverse reactions in a mouse model of oral squamous cell carcinoma treated with oxaliplatin at different time points during a day. Drug Des Devel Ther 2013; 7: 511-517.
[18] Abolmaali K, Balakrishnan A, Stearns AT, Rounds J, Rhoads DB, Ashley SW, Tavakkolizadeh A. Circadian variation in intestinal dihydropyrimidine dehydrogenase (DPD) expression: a potential mechanism for benefits of 5FU chrono-chemotherapy. Surgery 2009; 146: 269-273.
[19] Arif IS, Hooper CL, Greco F, Williams AC and Boateng SY. Increasing doxorubicin activity against breast cancer cells using PPARgamma-ligands and by exploiting circadian rhythms. Br J Pharmacol 2013; 169: 1178-1188.
[20] Liu H, Zhu Y, Zhang T, Zhao Z, Zhao Y, Cheng P, Li H, Gao H and Su X. Anti-tumor effects of atractylenolide I isolated from Atractylodes macrocephala in human lung carcinoma cell lines. Molecules 2013; 18: 13357-13368.
[21] Tampellini M, Filipski E, Liu XH, Lemaigre G, Li XM, Vrignaud P, Francois E, Bissery MC and Levi F. Docetaxel chronopharmacology in mice. Cancer Res 1998; 58: 3896-3904.
[22] Wang JL, Wu DW, Cheng ZZ, Han WZ, Xu SW and Sun NN. Expression of high mobility group box - B1 (HMGB-1) and matrix metalloproteinase-9 (MMP-9) in non-small cell lung cancer (NSCLC). Asian Pac J Cancer Prev 2014; 15: 4865-4869.
[23] Safranek J, Pesta M, Holubec L, Kulda V, Dreslerova J, Vrzalova J, Topolcan O, Pesek M, Finek J and Treska V. Expression of MMP-7, MMP-9, TIMP-1 and TIMP-2 mRNA in lung tissue of patients with non-small cell lung cancer (NSCLC) and benign pulmonary disease. Anticancer Res 2009; 29: 2513-2517.
[24] Jin Y, Li JP, Tang LY, Chen JN, Feng ZY, Liu Y, Zhou J and Shao CK. Protein expression and significance of VEGF, EGFR and MMP-9 in non-small cell lung carcinomas. Asian Pac J Cancer Prev 2011; 12: 1473-1476.

[25] Shao W, Wang W, Xiong XG, Cao C, Yan TD, Chen G, Chen H, Yin W, Liu J, Gu Y, Mo M and He J. Prognostic impact of MMP-2 and MMP-9 expression in pathologic stage IA non-small cell lung cancer. J Surg Oncol 2011; 104: 841-846.

[26] Hegedus C, Truta-Feles K, Antalffy G, Varady G, Nemet K, Ozvegy-Laczka C, Keri G, Orfi L, Szakacs G, Settleman J, Varadi A and Sarkadi B. Interaction of the EGFR inhibitors gefitinib, vandetanib, pelitinib and neratinib with the ABCG2 multidrug transporter: implications for the emergence and reversal of cancer drug resistance. Biochem Pharmacol 2012; 84: 260-267.

[27] Chen YJ, Huang WC, Wei YL, Hsu SC, Yuan P, Lin HY, Wistuba, II, Lee JJ, Yen CJ, Su WC, Chang KY, Chang WC, Chou TC, Chou CK, Tsai CH and Hung MC. Elevated BCRP/ABCG2 expression confers acquired resistance to gefitinib in wild-type EGFR-expressing cells. PLoS One 2011; 6: e21428.

[28] Luo W, Liu Y, Zhang J, Luo X, Lin C and Guo J. Andrographolide inhibits the activation of NF-kappaB and MMP-9 activity in H3255 lung cancer cells. Exp Ther Med 2013; 6: 743-746.

[29] Zheng S, Chang Y, Hodges KB, Sun Y, Ma X, Xue Y, Williamson SR, Lopez-Beltran A, Montironi R and Cheng L. Expression of KISS1 and MMP-9 in non-small cell lung cancer and their relations to metastasis and survival. Anticancer Res 2010; 30: 713-718.

[30] Cohen MH, Williams GA, Sridhara R, Chen G, McGuinn WD Jr, Morse D, Abraham S, Rahman A, Liang C, Lostritto R, Baird A and Pazdur R. United States Food and Drug Administration Drug Approval summary: Gefitinib (ZD1839; Iressa) tablets. Clin Cancer Res 2004; 10: 1212-1218.

[31] Lee KH, Lee KY, Jeon YJ, Jung MH, Son C, Lee MK, Ryu JS, Yang SH, Lee JC, Kim YC and Kim SY. Gefitinib in Selected Patients with Pre-Treated Non-Small-Cell Lung Cancer: Results from a Phase IV, Multicenter, Non-Randomized Study (SELINE). Tuberc Respir Dis (Seoul) 2012; 73: 303-311.

[32] Chen XX, Sun H, Zhang L. Preliminary study of immunology mechanism of erlotinib-induced skin rash. Tumor 2011; 6: 542-545.

[33] Groblewska M, Mroczko B, Wereszczynska-Siemiatkowska U, Kedra B, Lukaszewicz M, Baniukiewicz A and Szmitkowski M. Serum interleukin 6 (IL-6) and C-reactive protein (CRP) levels in colorectal adenoma and cancer patients. Clin Chem Lab Med 2008; 46: 1423-1428.

[34] O'Malley D, Dinan TG and Cryan JF. Interleukin-6 modulates colonic transepithelial ion transport in the stress-sensitive wistar kyoto rat. Front Pharmacol 2012; 3: 190.

[35] Yang L, Su T, Lv D, Xie F, Liu W, Cao J, Sheikh IA, Qin X, Li L and Chen L. ERK1/2 mediates lung adenocarcinoma cell proliferation and autophagy induced by apelin-13. Acta Biochim Biophys Sin (Shanghai) 2014; 46: 100-111.

[36] Guo YH, Gao FH, Shi J, Yuan HH and Jiang B. [EGFR-ERK signaling pathway down-regulates miRNA-145 in lung cancer cells]. Zhonghua Zhong Liu Za Zhi 2013; 35: 187-192.

[37] Chang SC, Chang CY, Chang SJ, Yuan MK, Lai YC, Liu YC, Chen CY, Kuo LC and Yu CJ. Gefitinib-related interstitial lung disease in Taiwanese patients with non-small-cell lung cancer. Clin Lung Cancer 2013; 14: 55-61.

[38] Inoue A, Saijo Y, Maemondo M, Gomi K, Tokue Y, Kimura Y, Ebina M, Kikuchi T, Moriya T and Nukiwa T. Severe acute interstitial pneumonia and gefitinib. Lancet 2003; 361: 137-139.

[39] Murashige N, Tanimoto T and Oshima Y. Interstitial lung disease and gefitinib. N Engl J Med 2010; 363: 1578-1579.